Defence Science Journal, Vol. 69, No. 5, September 2019, pp. 517-527, DOI : 10.14429/dsj.69.12096

Template-free Micro-Doppler Signature Classification for Wheeled and Tracked Vehicles

Guanghu Jin*, Zhen Dong, Yongsheng Zhang, and Feng He

College of Electronic Science and Techonology, National University of Defense Technology, Changsha – 410 073, P. R. China
**E-mail: kingnudt@163.com*

ABSTRACT

The micro-Doppler signature is a time-varying frequency modulation imparted on radar echo caused by target's micro-motion. To save the trouble of constructing template in the target classification, this paper investigates the micro-Doppler signature of wheeled and tracked vehicles and proposes a template-free classification method. Firstly, the echo signature is established and the micro-Doppler difference of these two kinds of targets is analysed. Secondly, some new micro-Doppler features are defined according to their difference. The new defined features are micro-Doppler bandwidth, micro-Doppler expansion rate and micro-Doppler peak number. According to the characteristic of the micro-Doppler in the time-frequency domain, we proposed to realise the feature extraction by Hough transformation. Lastly, template-free subjection functions are proposed to define the relationship between the features and the vehicles. By fuzzy comprehensive evaluation, the final classification result is obtained by combining the subjection probabilities together. Experimental results based on the simulated data and measured data are presented, which prove that the algorithm has good performance.

Keywords: Template-free; Micro-Doppler; Feature extraction; Vehicle classification; Hough transform; Subjection probability

1. INTRODUCTION

Radar is a kind of microwave sensor which can exploit signal processing techniques for target detecting, imaging and classification[1-7]. When the microwave pulse transmit by the radar bounced from the moving targets, the carrier frequency of the signal will be shifted, which is known as the Doppler effect. The Doppler frequency shift reflects the velocity of the moving target. Target's micro-motions such as rotation, vibration may induce additional Doppler frequency modulations which are called the micro-Doppler effects[8-15].

Different kinds of targets may have different kinds of micro-motions, which makes micro-Doppler signature classification a promising means for identifying radar targets. The early studies are mainly focused on template-based classification of many kinds of targets, such as aircraft[1,16-17], human aquatic activity[3-7,18], missile defence[19-21] and ground vehicles[10,22-24]. Chen analysed the micro-Doppler modulation with a mathematical model in detail and introduced the micro-Doppler effect in radar[8-9]. Thayaparan proposed that different micro-motions generated different micro-Doppler signatures, which makes micro-motion feature extraction from micro-Doppler signal feasible[25]. Y. Kim proposed to utilise artificial neural network and support vector machine to identify human activities including running, walking, crawling via micro-motion features[7,18]. A. G. Stove proposed a vehicle discrimination algorithm based on the Doppler spectra[23]. Graeme E.S. proposed to discriminate wheeled and tracked vehicles based on template[24], in which the vehicles are classified based on the comparison between the template and measured data.

Wheeled and tracked vehicles are the most commonly used battlefield vehicles. They are often served in different military missions. Wheeled vehicles are often used for accomplishing transportation missions quickly. Meanwhile, tracked vehicles often serve in carrying heavy weapons in attack missions. These two kinds of vehicles have different mission types and threaten degrees. Therefore, it is important to discriminate their types. In the prevent research, the wheeled and tracked vehicles classification is often accomplished by supervision with template in Refs. 10, 22-24, which brings a lot of inconvenience in the application.

To save the trouble in template establishing, a template-free classification algorithm of wheeled and tracked vehicles is proposed based on micro-Doppler signature. Firstly, some micro-Doppler features including micro-Doppler bandwidth, micro-Doppler expansion rate and micro-Doppler peak number are defined. Then, subjection functions are proposed to define the relationship between the features and the vehicles. Lastly, a further classification via fuzzy comprehensive evaluation is implemented to combine the subjection probabilities obtained by different means. Some experiments are carried out to verify the proposed method. The experiment result shows that the method has good performance.

Received : 12 October 2017, Revised : 23 June 2019
Accepted : 31 July 2019, Online published : 17 September 2019

2. MICRO-MOTION MODEL OF WHEELED AND TRACKED VEHICLE

2.1 The Motion of the Target's Bulk and its Doppler Spectra

The geometry of airborne radar system observing the ground moving target is as shown in Fig. 1. The GMT moves in the ground plane. At time $\eta = 0$, it moves to $(x_0, y_0, 0)$. Meanwhile, the platform moves to $(0, 0, h)$. The vertical slant range of the target respect to the radar is defined as $R_c = \sqrt{{y_0}^2 + h^2}$.

The distance between the radar and target at time η can be expressed as

$$R(\eta) = \sqrt{h^2 + (v_a\eta - x_0 - v_x\eta)^2 + (y_0 + v_y\eta)^2} \tag{1}$$

The radar echo after matching filtering can be expressed as:

$$S_r(t,\eta) = w(t)\exp\left\{-j2\pi f_c\left(t - \frac{2R(\eta)}{C}\right)\right\} \tag{2}$$

The Doppler frequency is

$$f_\eta = \frac{1}{2\pi}\frac{d\phi}{d\eta} = \frac{2}{\lambda}\frac{dR}{d\eta} \tag{3}$$

Because

$$\frac{dR(\eta)}{d\eta} = \frac{1}{R(\eta)}\left\{(v_a - v_x)\left[(v_a - v_x)\eta - x_0\right] + v_y(y_0 + v_y\eta)\right\} \tag{4}$$

The Doppler frequency can be expressed as:

$$f_\eta = \frac{2}{\lambda R(\eta)}\left\{(v_a - v_x)\left[(v_a - v_x)\eta - x_0\right] + v_y(y_0 + v_y\eta)\right\} \tag{5}$$

Since the illuminating time on the target is not very long, the variation of $R(\eta)$ is not very remarkable. Therefore, the Doppler frequency can be seen as changing with time η linearly.

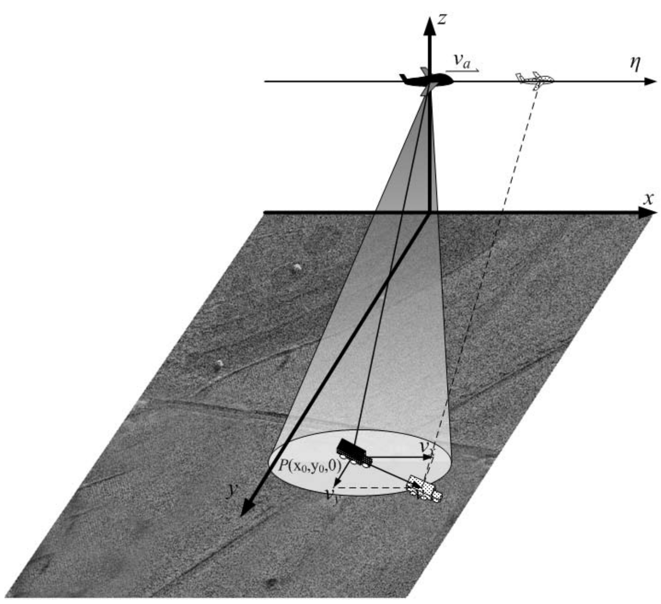

Figure 1. Target's motion under radar illumination

2.2 The Motion of the Vehicle's Wheel and its Doppler Spectra

The vehicle's wheel motion is as shown in Fig. 2. The velocity of the vehicle is v. The moving direction is $\overline{OB}$ which is in the xy plane. The wheel's radial length is r. The rotation speed is ω which is equal to $v/2\pi r$.

For a scattering center on the wheel, the velocity components along three axes are:

$$\begin{cases} v_x = -\omega r\sin(\omega\eta + \varphi_0)\cos\alpha - v_p \\ v_y = -\omega r\sin(\omega\eta + \varphi_0)\sin\alpha \\ v_z = \omega r\cos(\omega\eta + \varphi_0) \end{cases} \tag{6}$$

Therefore, the range can be expressed as

$$R(\eta) = \left[\begin{array}{l}\left(h - \omega r\eta\cos(\omega\eta + \varphi_0)\right)^2 + (v_p\eta - x_0 + \omega r\eta\sin(\omega\eta + \varphi_0) \\ \cos\alpha)^2 + (y_0 - \omega r\eta\sin(\omega\eta + \varphi_0)\sin\alpha)^2\end{array}\right]^{\frac{1}{2}} \tag{7}$$

The Doppler frequency is

$$\begin{aligned} f_\eta = \frac{2}{\lambda R(\eta)}&\left\{{v_p}^2\eta + \omega^2 r^2\eta - v_p x_0\right. \\ &+\left[h\omega^2 r\eta + \omega r(v_p\eta - x_0)\cos\alpha + v_p\omega r\eta\cos\alpha - y_0\omega r\sin\alpha\right]\sin(\omega\eta + \varphi_0) \\ &\left.+\left[-h\omega r - y_0\omega r\eta\sin\alpha + \omega^2 r\eta(v_p\eta - x_0)\cos\alpha\right]\cos(\omega\eta + \varphi_0)\right\} \end{aligned} \tag{8}$$

From the formula above it can be seen that the Doppler frequency of the wheel is the combination of polynomial functions and trigonometric functions.

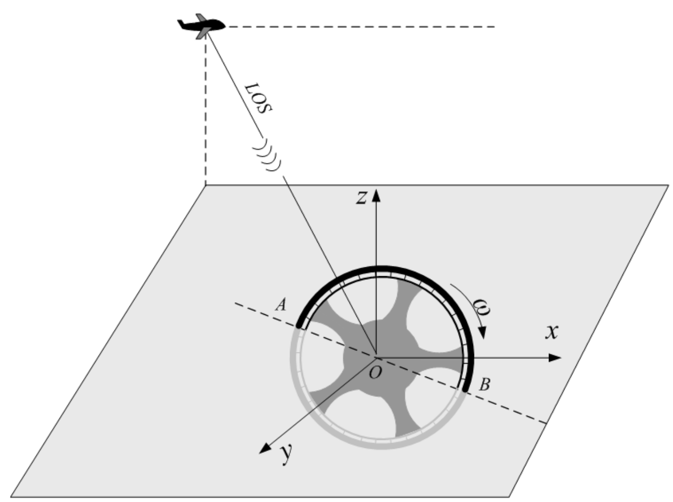

Figure 2. Vehicle's wheel motion model.

2.3 The Motion of the Vehicle's Track and its Doppler Spectra

The typical motion model of vehicle's track is as shown in Fig. 3.

The track is made up of several segments. Different segments have different motion style. Segment 1, 3, 5, 7 move straightly while segment 2, 4, 6, 8 rotate around different points. For rotation segments, the Doppler effect is similar with the wheel's. For scattering center on the top segment, its velocity is twice of the bulk's velocity, which can be divided as $(2v_x, 2v_y, 0)$. The range between radar and the scattering center is

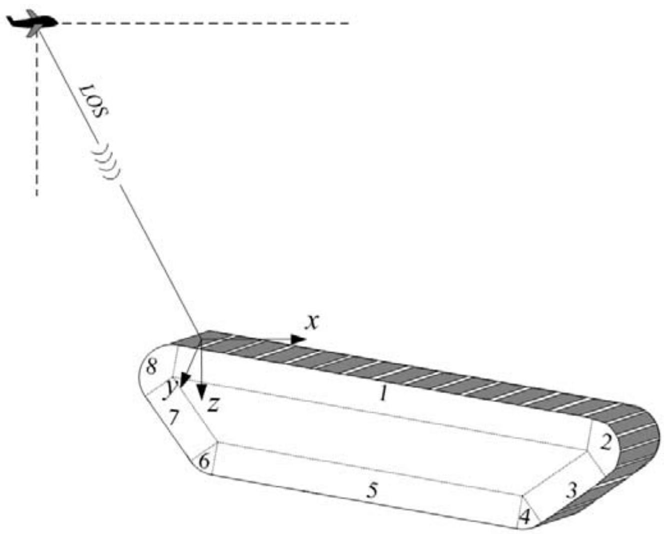

Figure 3. Vehicle's track motion model.

$$R(\eta)=\sqrt{\left(h-h_0\right)^2+(v_a\eta-x_0-2v_x\eta)^2+(y_0+2v_y\eta)^2} \quad (9)$$

Therefore, the Doppler frequency is:

$$f_\eta=\frac{2}{\lambda R(\eta)}\left\{(v_a-v_x)\left[(v_a-2v_x)\eta-x_0\right]+v_y(y_0+2v_y\eta)\right\} \quad (10)$$

For bottom segment, it is stationary relative to the background. The Doppler frequency is the same as the clutter. The range is:

$$R(\eta)=\sqrt{h^2+(v_a\eta-x_0)^2+y_0{}^2} \quad (11)$$

The Doppler frequency is:

$$f_\eta=\frac{2}{\lambda R(\eta)}\left(v_a{}^2\eta-v_a x_0\right) \quad (12)$$

For segment 3 and 7, the velocity can be divided into a component along the terrain surface and a component vertical to light of radar sight. Because latter component does not arise the range variation, it has no contribution to the Doppler shift. Only the former component will cause Doppler shift. Suppose that the velocity component in the ground plane is further divided into v_x' and v_y', the range is:

$$R(\eta)=\sqrt{h^2+(v_a\eta-x_0-v_x'\eta)^2+(y_0+v_y'\eta)^2} \quad (13)$$

Therefore, the Doppler frequency is:

$$f_\eta=\frac{1}{2\pi}\frac{d\phi}{d\eta}=\frac{2}{\lambda R(\eta)}\left\{(v_a-v_x')\left[(v_a-v_x')\eta-x_0\right]+v_y'(y_0+v_y'\eta)\right\} \quad (14)$$

For scattering centers on the track, they will pass through different segments. The Doppler frequency will change with the slow time. The Doppler frequency changing of one scattering point on the track is as shown in Fig. 4.

2.4 The Micro-Doppler of Wheeled and Tracked Vehicles

The spectra of vehicle are the combination of spectra of the bulk and the micro-Doppler spectra of the wheel or the track. Commonly, because the wheel is mainly made of rubber[10,24], the wheel's back-scattering is weak. Therefore, the wheeled vehicle's spectra are mainly made up of the bulk's spectra. But for tracked vehicle, the track is made of several metallic parts. The back-scattering is strong. The tracked vehicle's spectra are made up of the bulk's spectra and the track's spectra.

Simulations for wheeled and tracked vehicles are carried out. The center frequency of the radar is 10GHz. The incidence angle is 30º. The velocity of the carrier airplane is 200m/s. The velocity of the target is 13.9 m/s (about 50 km/h). Figure 5(a), 5(b) and 5(c) reveal the spectra of the vehicle's bulk, a wheel and a track. Figures 5(d) and 5(e) reveal the whole spectra of wheeled and tracked vehicles.

3. MICRO-DOPPLER FEATURE EXTRACTION

3.1 Micro-Doppler Instant Bandwidth

According to Fig. 5, we can see that the Doppler spectra of wheeled and tracked vehicles have many differences. If the difference can be characterised and quantified, the classification will be realistic. In this section, we define some new micro-Doppler features to reflect the difference. Hence, it will help to realise classification.

The first defined feature is micro-Doppler instant bandwidth. From the simulation and analysis above, we can

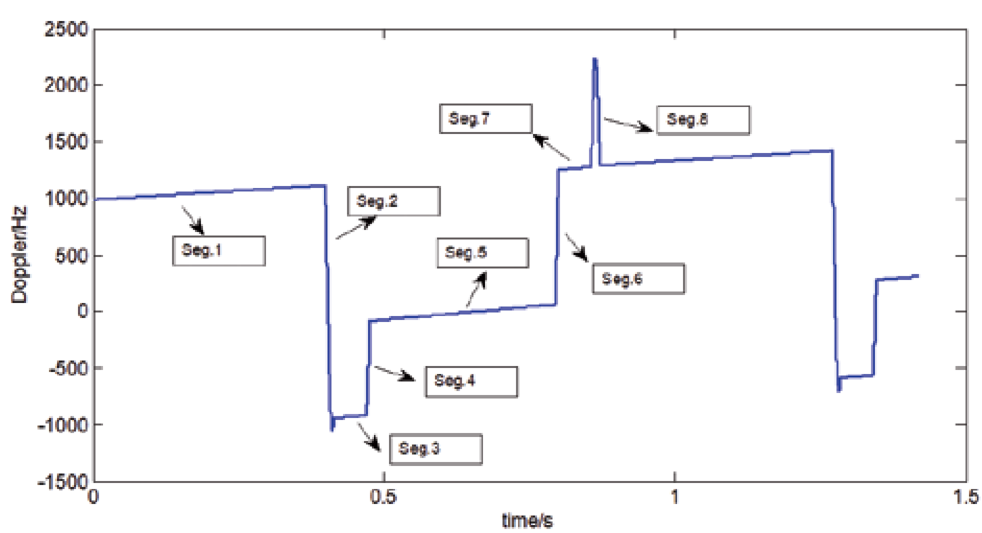

Figure 4. Doppler change of one scattering point on the track.

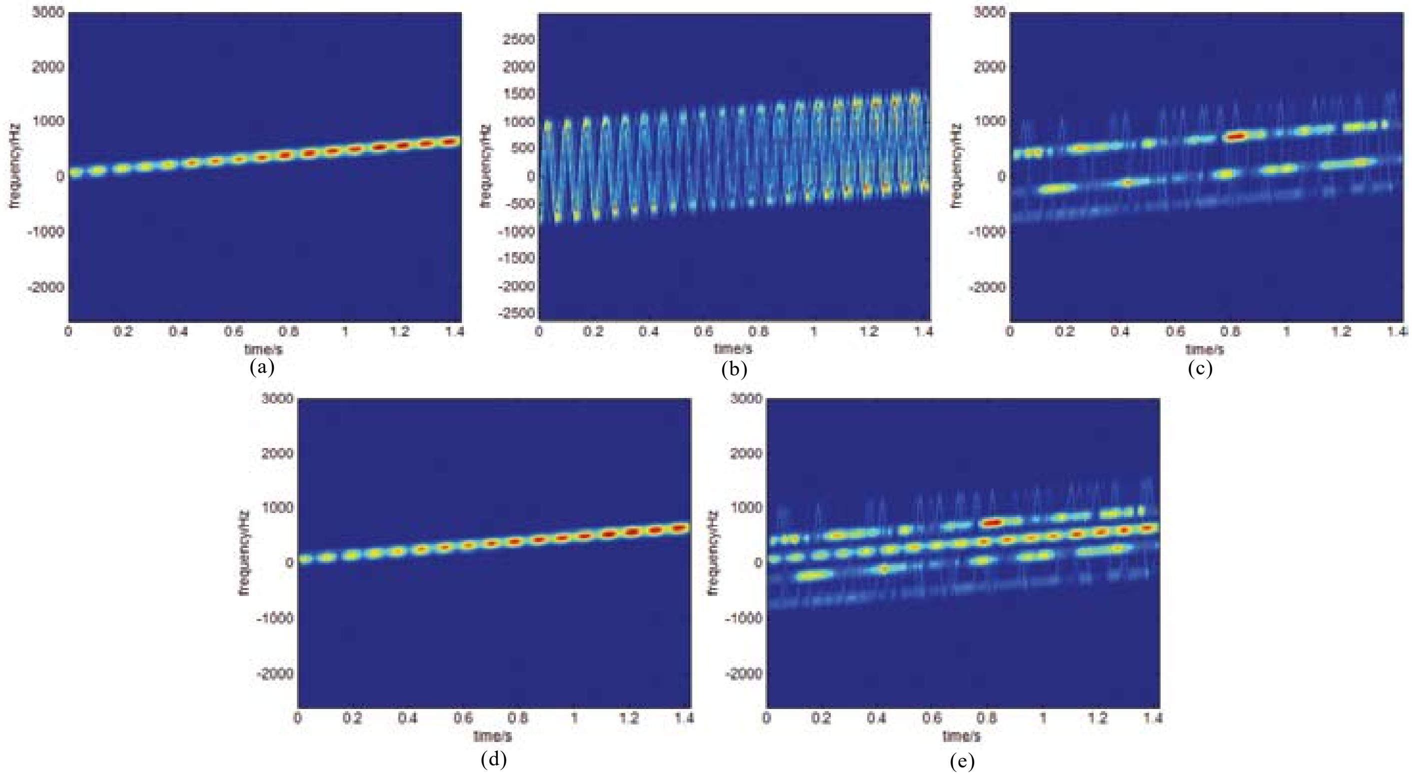

Figure 5. The spectra of the wheels, tracks and the vehicles: (a) bulk's, (b) wheel's, (c) track's, (d) wheeled vehicle's, and (e) tracked vehicle's.

see that the instant Doppler bandwidth of the wheeled vehicle has limited bandwidth. But for tracked vehicle, the instant Doppler bandwidth is much bigger.

Doppler frequency is the frequency shift of the echo respect to the frequency of the transmit pulse caused by the relative motion. For radar target, the Doppler frequency is

$$f_\eta = \frac{v \sin\theta}{C} f_c \tag{15}$$

Among above, squint angle θ is the angle between the radar sight and the moving direction. For a scattering center with fixed velocity, the echo is a single-frequency signal.

For wheeled vehicle, because the rubber wheel's back-scattering is weak, the Doppler spectra are mainly made up of the bulk's spectra[10,24]. Since the bulk's velocity is fixed, the instant Doppler difference is caused by the squint angle θ difference. For a target which is only several or tens of meters, the squint angles for all scattering centers are almost the same. Therefore, the instant Doppler frequency bandwidth is very small. Theoretically, the instant bandwidth is nearly zero. But considering the limitation of the frequency resolution in time-frequency transform, the instant bandwidth will not be zero. It is the reciprocal of the slow-time window width

$$B_{\eta,inst} = \frac{1}{T_m} \tag{16}$$

Among above, T_m is the slow-time window width used for the time-frequency transform.

For tracked vehicle, the Doppler spectra are much more complex. Besides strong back-scattering caused by the vehicle's bulk, the metallic track may cause strong back-scattering, too. For vehicle's bulk, the instant bandwidth is not very big. It is the same to the wheeled vehicles bulk which is expressed in Eqn (16). For scattering centers on the track, the velocity changes with the position variation along the track. It will cause many additional Doppler changes. The instant Doppler bandwidth will be much bigger compared with the wheeled vehicle.

For a target with fixed velocity, the maximum Doppler frequency is in accordance with the situation that the target comes near along the radar sight. The minimum Doppler frequency is in accordance with the situation that the target leaves away along the radar sight. Different scattering centers on different segments have different directions. Their Doppler frequency shifts have great difference. For the top segment whose velocity is $2v$, the Doppler frequency is

$$f_{\eta,top} = \frac{2}{\lambda}\frac{dR}{d\eta} = \frac{2\left[(v_a\eta - x_0 - 2v_x\eta)(v_a - 2v_x) + (y_0 + 2v_y\eta)2v_y\right]}{\lambda R(\eta)} \tag{17}$$

For the bottom segment whose velocity is 0, the Doppler frequency is

$$f_{\eta,bottom} = \frac{2}{\lambda}\frac{dR}{d\eta} = \frac{2(v_a\eta - x_0)v_a}{\lambda R(\eta)} \tag{18}$$

The instant Doppler bandwidth $B_{\eta,inst}$ is the difference between the Doppler of all segments. It should be bigger than

$$B_{\eta,inst} \geq f_{\eta,top} - f_{\eta,bottom} = \frac{2\left[-2v_x\eta(v_a - 2v_x) + (y_0 + 2v_y\eta)2v_y\right]}{\lambda R(\eta)} \tag{19}$$

Summarising the analysis above, it can be concluded that:

(i) Because the wheels are mostly made up of rubber, the Doppler spectra are mostly made of the bulk's Doppler. The wheeled vehicle's micro-Doppler phenomenon cannot be observed. While the velocity of the vehicle nearly does not change in short time interval, the instant Doppler bandwidth is nearly zero. Considering the frequency resolution limitation in time-frequency transform, the actual instant Doppler bandwidth is the reciprocal of the slow-time window width used in time-frequency transform.

(ii) Unlike the wheel, the track of the vehicle is metallic. The back-scattering of the track is strong. Due to the fact that different parts on the track have different Doppler shift, the instant Doppler bandwidth is much bigger.

3.2 Micro-Doppler Expansion Rate

If the instant Doppler bandwidth is used for target classification directly, its real value should be known in advance. That means the template should be established. To save the trouble in template establishing, a new feature named micro-Doppler Expansion Rate (MDER) is defined, which will help to realise template-free classification.

Actually, because of the limited window's width for time-frequency transform, the Doppler bandwidth resolution is limited. Commonly, it is defined as the width when the energy declined by -3dB. The micro-Doppler Expansion Rate is defined as the rate of the instant Doppler bandwidth to the Doppler bandwidth resolution.

$$MDER = \frac{B_{\eta,inst}}{B_{res}} \tag{20}$$

Among above, $B_{res} = 1/T_m$ and T_m is the window width of slow time in the time-frequency transform.

3.3 Micro-Doppler Peak Number of the Micro-Doppler Spectra

It has been mentioned above that some segments of the track have fixed velocity. Because the velocity of the SAR platform is much bigger than target velocity, the Doppler chirp rates are mainly decided by the platform speed. Commonly, this velocity is fixed and very stable, which means that the Doppler spectra of these segments change with slow time nearly linearly. If they are projected along the Doppler chirp direction, one interesting phenomenon will appear which is that the spectra are projected into some isolated peaks. Each segment spectra will be projected into one peak. Therefore, in the project result of the tracked vehicle's spectra, there will be few peaks. But for wheeled vehicle, because the spectra are mostly caused by the vehicle bulk, the spectra project will have only one peak. Here the linear component quantity after integration is defined as micro-Doppler peak number (MDPN).

3.4 Feature Extraction based on Hough Transform

Micro-Doppler bandwidth, micro-Doppler expansion rate and micro-Doppler peak number are defined based on the instant Doppler spectra $S(t_m, f_\eta)$. From Fig. 5, we can see that the Doppler spectra changes with slow-time. To extract the features defined above, integration should be carried out.

$$A_\theta(f_p) = \int_{f_\eta / t_m = \tan\theta} S(t_m, f_\eta) df_\eta \tag{21}$$

The best integration direction is in accordance with the bulk's Doppler changing direction. Based on Formula (4), the second derivate of $R(\eta)$ is

$$\left.\frac{d^2 R(\eta)}{d\eta^2}\right|_{\eta=0} = \frac{(v_a - v_x)^2}{R_c} - \frac{(x_0 v_x + y_0 v_y - x_0 v_a)^2}{R_c^{\ 3}} \tag{22}$$

Therefore, the chirp rate is

$$K_a = \frac{2}{\lambda}\frac{1}{R_c^{\ 3}}\left[R_0^{\ 2}(v_a - v_x)^2 - (x_0 v_x + y_0 v_y - x_0 v_a)^2\right] \tag{24}$$

Since $R_c \gg \frac{x_0 v_x + y_0 v_y - x_0 v_a}{v_a - v_x}$, the chirp rate can be approximated as

$$K_a = \frac{2}{\lambda}\frac{1}{R_c}(v_a - v_x)^2 \tag{25}$$

Unfortunately, we do not know the target motion parameters. The integration direction should be obtained first. This estimation can be done by Hough transform which realise integral under different directions. When the integration direction is in accordance with the Doppler changing direction, the Doppler spectra will be projected into a limited bandwidth. If the direction has errors, the result will be expanded. The integration along the right and the wrong direction are as shown in Fig. 6.

From Fig. 6, we can see that the energy will be more centralised under the right integral direction. Next, an evaluate function is defined to help seeking the integral direction:

$$P(\theta) = \frac{\sum\left\{A_\theta^{\ 2}(f_p) - E^2\left[A_\theta(f_p)\right]\right\}}{E^2\left[A_\theta(f_p)\right]} \tag{26}$$

When the integral direction is in accordance with the Doppler chirp rate, $P(\theta)$ will reach the maximum value. Therefore, the Doppler changing direction is in accordance with the maximum position of $P(\theta)$.

$$\hat{\theta} = \arg\left\{\max P(\theta)\right\} \tag{27}$$

After the instant Doppler accumulation $A_{\hat{\theta}}(f_p)$ is obtained, we can get the micro-Doppler bandwidth, micro-Doppler expansion rate and micro-Doppler peak number easily according to their definitions.

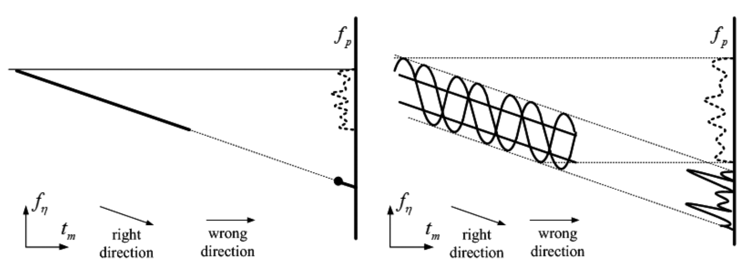

(a) (b)

Figure 6. Spectra integration along Doppler change direction: (a) wheeled and (b) tracked.

4. TEMPLATE-FREE CLASSIFICATION

4.1 Vehicles Classification based on Micro-Doppler Bandwidth Expansion Rate

To realise template-free classification, we propose using subjection function to define the relationship between micro-Doppler feature and target type. For wheeled vehicle, the Doppler bandwidth expansion rate should be about 1.0. But for tracked vehicle, the expansion rate will be much bigger than 1.0. According to this fact, a new subjection function is defined to reveal the probability that the observed target belongs to a certain type. The probability subjected to wheel type is

$$P_{\in wheel}(MDER)=\begin{cases}1, MDER<1\\ \dfrac{\cos\left[\pi\times\left(1-e^{-\frac{MDER-1}{2}}\right)\right]+1}{2}, MDER\geq 1\end{cases} \tag{28}$$

The probability subjected to track type is

$$P_{\in track}(MDER)=\begin{cases}0, MDER<1\\ \dfrac{1-\cos\left[\pi\times\left(1-e^{-\frac{MDER-1}{2}}\right)\right]}{2}, MDER\geq 1\end{cases} \tag{29}$$

The function can be expressed as the curves in Fig. 7.

The designed subjection function reveals the relationship between MDER and target type. From the Fig. 7, we can see that the probability subject to wheel type will be 1 only when MDER is about 1.0. If MDER is much bigger than 1.0, the probability subject to wheel type will drop down rapidly and the probability subject to track type will increase remarkably.

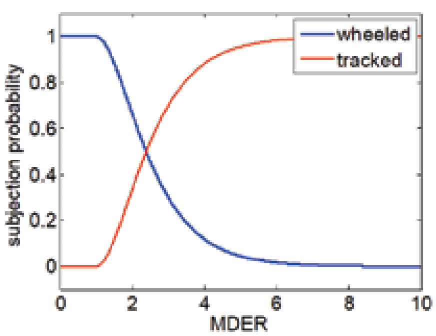

Figure 7. The subjection function to expansion rate.

4.2 Vehicles Classification based on Micro-Doppler Peak Number

For tracked vehicle, the Doppler spectra consist of a few linear components caused by the top parts, the bottom parts, the left parts, the right parts and the vehicles' bulk. So, the quantity may be about 5 or more. But for wheeled vehicle, there is only one main component which is the bulk's spectra. Here we defined another subjection function based on micro-Doppler peak number. The probability subjected to wheel type is

$$P_{\in wheel}(MDPN)=\begin{cases}1, MDPN=1\\ 0, MDPN>1\end{cases} \tag{30}$$

The probability subjected to track type is

$$P_{\in track}(MDPN)=\begin{cases}0, MDPN=1\\ 1, MDPN>1\end{cases} \tag{31}$$

The function can be expressed as the curves in Fig. 8.

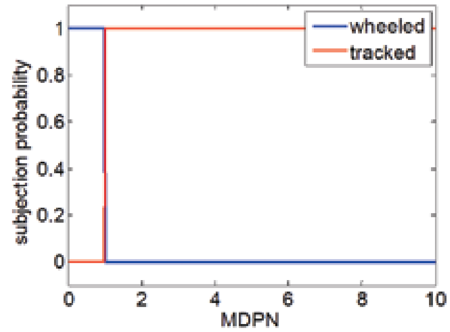

Figure 8. The subjection function to micro-Doppler peak number.

4.3 Subjection Probability Combination based on Fuzzy Comprehensive Evaluation

For vehicles classification, the probability is obtained based on MDER and MDPN. By combining the probabilities through fuzzy comprehensive evaluation, the final result can be obtained.

There are two factor for evaluation which are MDER and MDPN, and two evaluation result which are:

(i) It belongs to wheeled type and
(ii) It belongs to tracked type.

For each evaluation factor, the evaluation result is r_{ij} which forms the evaluation matrix $R(r_{ij})_{2\times 2}$. In the evaluation process, different evaluation factors have different impact weights. The weighs can be assigned according to the experience. Here, a_1 is the weight for MDER and a_2 is the weight for MDPN. The weights satisfy $\sum_{i=1}^{m} a_i=1$ ($a_i>0$, $i=1,2$). The final result P after fuzzy comprehensive evaluation is

$$P=[p_1,p_2]=[a_1,a_2]\begin{bmatrix}r_{11} & r_{12}\\ r_{21} & r_{22}\end{bmatrix} \tag{32}$$

Among above, p_1 represents the probability that the target belongs to wheeled type and p_2 represents the probability that the target belongs to tracked type.

5. EXPERIMENTS AND RESULTS

5.1 Experiments based on Simulated Data

The presented algorithm is tested using the simulated or tested data. The first experiment is based on simulated data. Suppose that the radar works at 10 GHz. The incidence angle is 30º. The velocity of the plane is 200 m/s. The velocity of the target is 13.9 m/s (about 50 km/h). The echoes are simulated. The Doppler spectra are as shown in Fig. 5. To extract the micro-Doppler features, Hough transforms are executed. The results are as shown in Fig. 9.

According to Section 3.4, the integration result along the Doppler change direction as shown in Fig. 10.

We can see from the figure, that tracked and wheeled vehicle have different MDER and MDPN. Experiments with different moving directions are carried out. The micro-Doppler feature extraction results are as listed in Table 1.

From Table 1, it can be seen that the tracked vehicle has a much bigger instant Doppler bandwidth. Therefore, MDER is much bigger. Meanwhile, there are more peaks in the integration result.

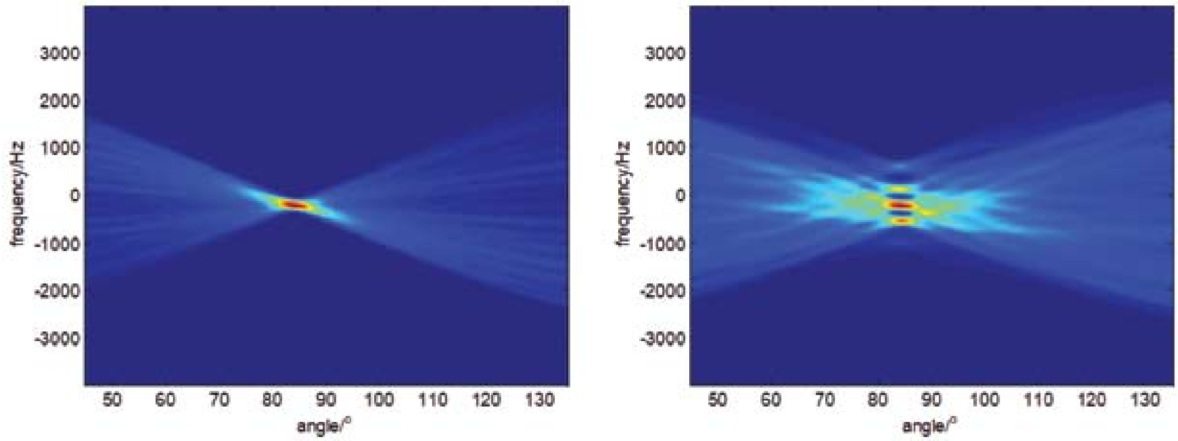

(a) (b)

Figure 9. Hough transform results of the wheeled and tracked vehicle's spectra: (a) wheeled vehicle and (b) tracked vehicle.

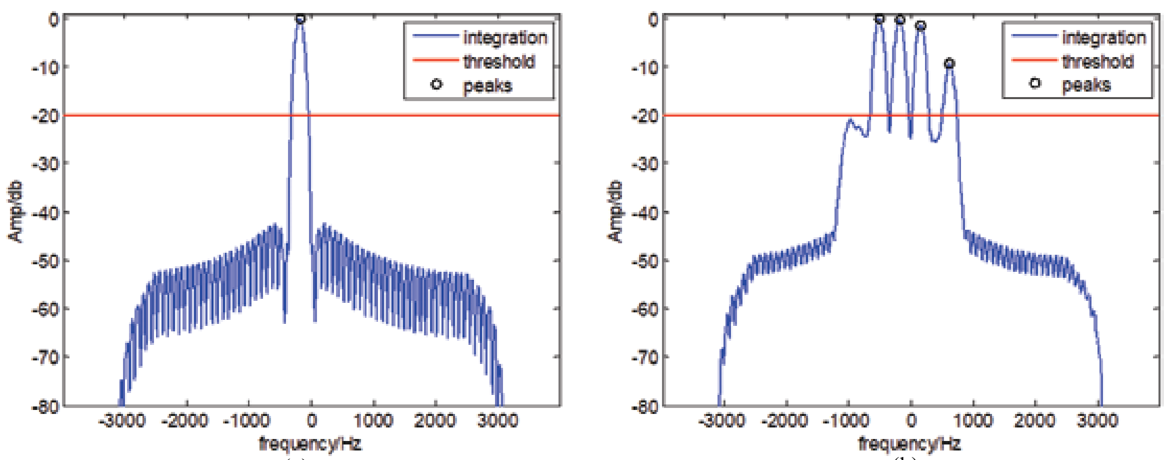

(a) (b)

Figure 10. Integration results and Micro-Doppler feature extraction: (a) Wheeled vehicle and (b) Tracked vehicle.

For target with velocity 50 km/h under different moving direction, the subjection probability based on the instant bandwidth is obtained by formula (28) and (29). The results are as listed in Table 2.

Similarly, the subjection probabilities based on the MDPN are obtained by formula (30) and (31). The results as are listed in Table 3.

For target with velocity 50 km/h under different moving direction, the subjection probability after fuzzy comprehensive evaluation is as listed in Table 4.

From Tables 2-4, it can be seen that the wheeled vehicles are classified as wheeled type with high probability and the tracked vehicles are classified as wheeled type with high probability, too.

More experiments for targets with different velocity are carried out. Targets with velocity 5 m/s, 10 m/s, 15 m/s, 20 m/s are classified, the subjection probabilities are as listed in the Table 5.

It can be seen from Table 5 that the proposed template-free classification algorithm has good performance for targets with different velocity.

Table 1. Micro-Doppler feature extraction result

Motion direction	Wheeled vehicle			Tracked vehicle		
	IDBW(Hz)	MDER	MDPN	BW(Hz)	MDER	MDPN
0°	268.4233	1.5145	1	1370.3714	7.7320	3
45°	268.6592	1.5159	1	1371.5761	7.7389	4
90°	268.9161	1.5173	1	1563.9596	8.8244	5
135°	269.194	1.5189	1	1381.3904	7.7943	4
180°	276.585	1.5606	1	1312.0056	7.4028	3
225°	276.2781	1.5589	1	1331.8021	7.5145	4
270°	268.9161	1.5173	1	1592.2666	8.9841	5
315°	268.6592	1.5159	1	1399.8561	7.8985	4

Table 2. Subjection probability based on the instant bandwidth

Motion direction	Wheeled vehicle		Tracked vehicle	
	As wheeled	As tracked	As wheeled	As tracked
0°	0.8622	0.1378	0.0039	0.9961
45°	0.8778	0.1222	0.0025	0.9975
90°	0.8772	0.1228	0.0010	0.9990
135°	0.8766	0.1234	0.0028	0.9972
180°	0.8597	0.1403	0.0041	0.9959
225°	0.8604	0.1396	0.0037	0.9964
270°	0.8772	0.1228	0.0008	0.9992
315°	0.8778	0.1222	0.0025	0.9975

Table 3. Subjection probability based on the MDPN

Motion direction	Wheeled vehicle		Tracked vehicle	
	As wheeled	As tracked	As wheeled	As tracked
0°	1	0	0	1
45°	1	0	0	1
90°	1	0	0	1
135°	1	0	0	1
180°	1	0	0	1
225°	1	0	0	1
270°	1	0	0	1
315°	1	0	0	1

Table 4. Subjection probability after fuzzy comprehensive evaluation

Motion direction	Wheeled vehicle		Tracked vehicle	
	As wheeled	As tracked	As wheeled	As tracked
0°	0.9311	0.0689	0.0027	0.9973
45°	0.9389	0.0611	0.0012	0.9988
90°	0.9386	0.0614	0.0005	0.9995
135°	0.9383	0.0617	0.0014	0.9986
180°	0.9298	0.0702	0.0020	0.9980
225°	0.9302	0.0698	0.0018	0.9982
270°	0.9386	0.0614	0.0004	0.9996
315°	0.9389	0.0611	0.0012	0.9988

5.2 Experiments based on Measured Data

Another experiment based on measured data. There are five targets which are called No. 1 to No. 5. Four targets from No. 1 to No. 4 are tracked targets. No. 5 is a wheeled target. Neglecting the spectra among the starting and braking time, during the time that the velocity is stable, we can see that the Doppler spectra are very similar with our simulation. It is proved that our micro-Doppler analyses and simulations are right.

In the experiments[27], the target velocity is not fixed. Compensation is done to get the spectra under fixed velocity. The spectra also contain the clutter spectra and the imperfections, and they are filtered out in our pre-processing. The results after our compensation and clutter suppress are as shown in left and the middle columns in Fig. 11. And their integration results along the Doppler change direction are as shown in the right column in Fig. 11.

Table 5. Subjection probability for targets with different velocity

Velocity (m/s)	Wheeled vehicle		Tracked vehicle	
	As wheeled	As tracked	As wheeled	As tracked
5	0.9305	0.0695	0.0867	0.9133
10	0.9389	0.0611	0.0019	0.9981
15	0.9389	0.0611	0.0009	0.9991
20	0.9392	0.0608	0.0001	0.9999

We use the result above to realise wheeled and tracked vehicle classification without template. In the right column of Fig. 11, sometimes small peaks appear at zero Doppler position because of the clutter spectra removing incomplete. They are neglected in the feature extraction. The extracted Micro-Doppler features are as listed in Table 6.

Table 6. Micro-Doppler feature extraction result

Target No.	BW (Hz)	MDER	MDPN
1	615.37	18.65	12
2	684.91	20.75	11
3	654.10	19.8212	10
4	702.08	21.28	7
5	34.42	1.04	1

Based on the extracted micro-Doppler features, classification is executed. The results are as listed in Table 7.

From the result in Table 7, we can see that the proposed template-free classification algorithm can classify the wheeled and tracked targets effectively.

6. CONCLUSIONS

In this paper, the micro-motion of military vehicles based on the point-scattering model is established and the Doppler spectra of the wheeled and tracked vehicles are analysed. According to the analysis, the micro-Doppler component induced by the track or wheel can be considered as an important feature. We propose to extract three features including micro-Doppler bandwidth, micro-Doppler expansion rate and micro-Doppler peak number to realise target classification. Subjection functions based on these features are proposed to define the relationship between these features and the vehicle types. A further processing via fuzzy comprehensive evaluation is implemented to combine the subjection probabilities together. Experiment results based on the simulated and measured data verified that the algorithm has good performance.

Table 7. Subjection probability for wheeled and tracked vehicle classification

Target No.	Based on MDER		Based on MDPN		Based on fuzzy comprehensive evaluation	
	Wheeled	Tracked	Wheeled	Tracked	Wheeled	Tracked
1	5.33e-8	1	0	1	2.67e-8	1
2	6.53e-9	1	0	1	3.26e-9	1
3	1.65e-8	1	0	1	8.24e-9	1
4	3.84e-9	1	0	1	1.92e-9	1
5	0.999	9.67e-4	1	0	0.9995	4.84e-4

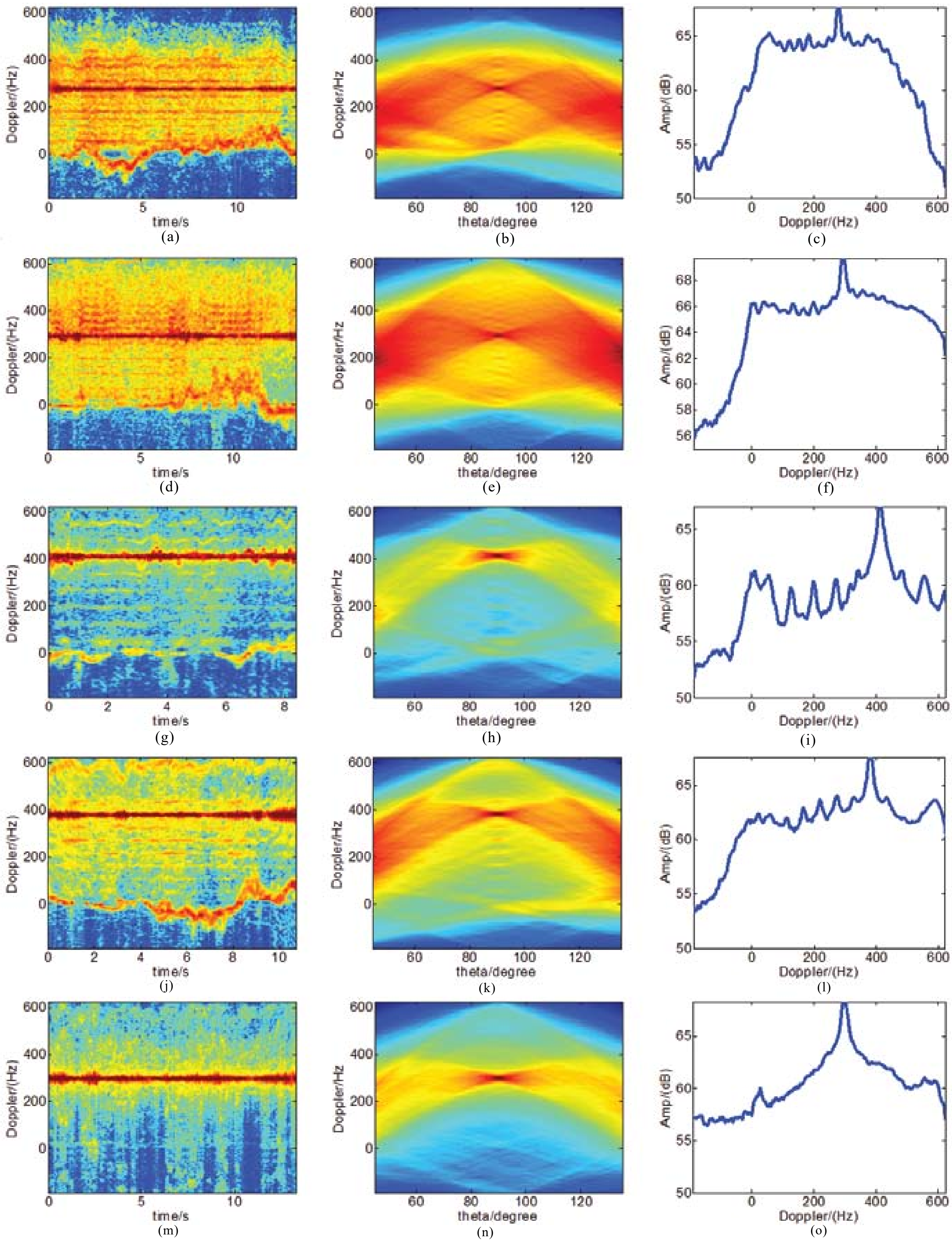

Figure 11. Feature extraction based on integration result: (a, d, g, j, m) Spectra of Target No. 1., (b, e, h, k, n) Hough transform result and (c, f, i, l, o) Integration result.

REFERENCES

1. Kim, B. K.; Kang, H.-S; & Park, S.-O. Drone classification using convolutional neural networks with merged Doppler images. *IEEE Geosci. Remote Sens. Lett*., 2017, **14**(1), 38-42.
doi:10.1109/LGRS.2016.2624820
2. Du, L.; Ma, Y.; Wang, B. & Liu, H. Noise-robust classification of ground moving targets based on time-frequency feature from micro-Doppler signature. *IEEE Sens. J.,* 2014, **14**(8), 2672-2682.
doi:10.1109/JSEN.2014.2314219
3. Nanzer, J. A. A review of microwave wireless techniques for human presence detection and classification. IEEE Trans. Microw. Theory Tech., 2017, **65**(5), 1780-1794.
doi:10.1109/TMTT.2017.2650909
4. Tivive, F. H. C.; Phung, S. L. & Bouzerdoum, A. Classification of micro-doppler signatures of human motions using log-gabor filters. *IET Radar Sonar Navig.*, 2015, **9**(9), 1188-1195.
doi:10.1049/iet-rsn.2015.0113
5. F. Fioranelli; M. Ritchie & H. Griffiths. Centroid features for classification of armed/unarmed multiple personnel using multistatic human micro-Doppler. *IET Radar Sonar Navig.*, 2016, **10**(9), 1702-1710.
doi:10.1049/iet-rsn.2015.0493
6. Karabacak, C.; Gürbüz, S. Z.; Gürbüz, A.C.; Guldogan, M.B.; Hendeby, G. & Gustafsson, F. Knowledge exploitation for human micro-doppler classification. *IEEE Geosci. Remote Sens. Lett.*, 2015, **12**(10), 2125-2129.
doi:10.1109/LGRS.2015.2452311
7. Kim, Y. & Moon, T. Human detection and activity classification based on micro-doppler signatures using deep convolutional neural networks. *IEEE Geosci. Remote Sens. Lett.*, 2016, **13**(1), 8-12.
doi:10.1109/LGRS.2015.2491329
8. V. C. Chen; F. Li; S.-S. Ho & H. Wechsler. Analysis of micro-Doppler signatures. *IEE Proc.-Radar Sonar Navig.* 2003, **150**(4), 271-276.
doi: 10.1049/ip-rsn:20030743
9. Chen, V. C.; Li, F.; Ho, S.-S. & Wechsler, H. Micro-Doppler effect in radar: Phenomenon, model, and simulation study. *IEEE Trans. Aerosp. Electron. Syst.* 2006, **42**(1), 2-21.
doi: 10.1109/TAES.2006.1603402
10. Yanbing, L.; Lan, D. & Hongwei, L. Hierarchical classification of moving vehicles based on empirical mode decomposition of micro-Doppler signatures. I*EEE Trans. Geosci. Remote Sens.,* 2013, **51**(5), 3001-3013.
doi: 10.1109/TGRS.2012.2216885
11. Rüegg, M. ; Meier, E. & Nüesch, D. Vibration and rotation in millimeter wave SAR. *IEEE Trans. Geosci. Remote Sens.* 2007, **45**(2), 293-304.
doi: 10.1109/TGRS.2006.887025
12. Cunsuo, P.; Yan, H.; Huiling, H.; Shengheng, L. & Nan, Z. Micro-Doppler signal time-frequency algorithm based on STFRFT. *Sensors,* 2016, **16**(10), 1559.
doi:10.3390/s16101559
13. Chen, V. C. Doppler signatures of radar backscattering from objects with micro-motions. *In* IET Signal Processing in Special Issue on Signal Processing Techniques for ISAR and Feature Extraction, 2008, **2**, 291-300.
doi:10.1049/iet-spr:20070137
14. Liu, Y. X. ; Li, X. & Zhuang, Z. W. Estimation of micro-motion parameters based on micro-Doppler. *IET Signal Process.*, 2010, **4**(3), 213-217.
doi:10.1049/iet-spr.2009.0042
15. Sun, H. & Su, S. Micro-Doppler frequency estimation based on radon-wigner transform. *Def. Sci. J.*, 2014, **64**(1), 85-87.
doi:10.14429/dsj.64.2980
16. Sun, H. Inverse Synthetic Aperture radar imaging for micro-motion target with rotating parts. *Def. Sci. J.*, 2013, **63**(5), 521-523.
doi:10.14429/dsj.63.4087
17. Yuan, B.; Chen, Z. & Xu, S. Micro-Doppler analysis and separation based on complex local mean decomposition for aircraft with fast-rotating parts in ISAR imaging. *IEEE Trans. Geosci. Remote Sens.*, 2014, **52**(2), 1285-1298.
doi:10.1109/TGRS.2013.2249588
18. Kim, Y. & Ling, H. Human activity classification based on micro-Doppler signatures using a support vector machine. *IEEE Trans. Geosci. Remote Sens.* 2009, **47**(5), 1328-1337.
doi: 10.1109/TGRS.2009.2012849
19. Sun, H.; Liu, Z. & Xue, N. Ballistic missile warhead recognition based on micro-Doppler frequency. *Def. Sci. J.*, 2008, **58**(6), 705-709.
20. Gao, H.; Xie, L.; Wen, S. & Kuang, Y. Micro-Doppler signature extraction from ballistic target with micro-motions. *IEEE Trans. Aerosp. Electron. Syst.,* 2010, **46**(4), 1969-1982.
doi:10.1109/TAES.2010.5595607
21. Persico, A.R.; Clemente, C.; Gaglione, D.; Ilioudis, C. V.; Cao, J. ; Pallotta, L. ; Maio, A. D.; Proudler, I. & Soraghan, J.J. On model, algorithms, and experiment for micro-Doppler-based recognition of ballistic targets. *IEEE Trans. Aerosp. Electron. Syst.,* 2017, **53**(3), 1088-1108.
doi:10.1109/TAES.2017.2665258
22. Chen, G. & Zhang, L. Micro-Doppler features analysis of the wheeled vehicle and the tracked vehicle. *Sensors & Transducers,* 2013, **158**(11), 326-331.
23. Stove, A. G. & Sykes, S. R. A Doppler-based target classifier using linear discriminants and principle components. *In* International Conference on Radar. 2003, Adelaide, 171-176.
doi: 10.1109/RADAR.2003.1278734
24. Graeme, E. S.; Karl, W. & Chris, J. B. Template based micro-Doppler signature classification. 3rd European Radar Conference. 2006, Manchester, 158-161.
doi: 10.1109/EURAD.2006.280298
25. Thayaparan, T.; Abrol, S.; Riseborough, E. ; Stankovic, L. ; Lamothe, D. & Duff, G. Analysis of radar micro-Doppler signatures from experimental helicopter and human data. *IET Radar, Sonar Navig*. 2007, **1**(4), 289-299.
doi:10.1049/iet-rsn:20060103

FUNDING

This work was supported by the National Natural Science Foundation of China under Grant numbers 61501474 and 61771478.

CONTRIBUTORS

Dr Guanghu Jin was born in Anhui, China, in February 1980. He received the BE, ME and PhD in electronics and information engineering from National University of Defense Technology, Changsha, in 2002, 2004 and 2009, respectively. He is currently an associate professor with the College of Electronic Science and Technology, National University of Defense Technology. His research interests include synthetic aperture radar (SAR), inverse SAR, and radar target recognition.
In the present study, he has been mainly responsible for overall signal processing technology development.

Dr Zhen Dong was born in Anhui, China, in September 1973. He received the PhD in electronics and information engineering from National University of Defense Technology, Changsha in 2001. He is currently a professor with the College of Electronic Science and Technology, National University of Defense Technology. His recent research interests include SAR system design and processing, Ground Moving Target Indication (GMTI), and digital beam-forming.
In the present study, he is involved in micro-Doppler feature extraction.

Dr Yongsheng Zhang was born in Inner Mongolia, China, in December 1977. He received the PhD in electronics and information engineering from National University of Defense Technology in 2007. He is currently an associate professor with the College of Electronic Science and Technology, National University of Defense Technology. His current major research interests include SAR system design and SAR data processing.
In the present study, he is involved in experiment.

Dr Feng He was born in Hubei, China, in October 1976. He received the BS and PhD in signal processing from National University of Defense Technology, Changsha, in 1998 and 2005, respectively. He is currently an associate professor with the College of Electronic Science and Technology, National University of Defense Technology. His current major research interests include SAR processing, digital beam-forming, space-time adaptive processing, and inverse SAR.
In the present study, he is involved in template-free classification.